Inorganica Chimica Acta 362 (2009) 136–142

Contents lists available at ScienceDirect

Inorganica Chimica Acta

journal homepage: www.elsevier.com/locate/ica

Remarkable chiral and luminescent properties of novel Yb(III) and Eu(III) complexes containing BINAPO ligand

Md. Abdus Subhan [a,*], Yasuchika Hasegawa [b], Takayoshi Suzuki [c], Sumio Kaizaki [c], Yanagida Shozo [b]

[a] Department of Chemistry, Shah Jalal University of Science and Technology, Sylhet, Bangladesh
[b] Department of Material and Life Science, Faculty of Engineering, Osaka University, Osaka, Japan
[c] Department of Chemistry, Faculty of Science, Osaka University, Osaka, Japan

ARTICLE INFO

Article history:
Received 2 September 2007
Received in revised form 29 January 2008
Accepted 11 March 2008
Available online 23 March 2008

Keywords:
Circular dichroism
Dissymmetry factors
Red emission
Lanthanide
Chirality

ABSTRACT

Lanthanide complexes are of great importance for their prospective applications in wide range of science and technology. Chiral lanthanide complexes can constitute stereo-discriminating probes in biological media, owing to the luminescent properties of the rare-earth ions. Sensitized emission with narrow bandwidth, having fast radiation rate and high emission quantum efficiency are the main perspective for synthesizing the complexes. Attention has been given on remarkable chirality with high dissymmetry factors ($g = \Delta\varepsilon_{ext}/\varepsilon_{max}$) of the complexes. For this purpose, beta-diketonato ligands with chiral BINAPO (1,1′-binapthyl phosphine oxide) ligand were chosen to achieve the goal. The complexes [Ln(TFN)$_3$(*S*-BINAPO)](TFN = 4,4,4-trifluoro-1(2-napthyl)-1,3-butanedione), [Ln(HFT)$_3$(*S*-BINAPO)] (HFT = 4,4,5,5,6,6,6-heptafluoro-1-(2-thienyl)-1,3-hexanedione) and [Ln(HFA)$_3$(*S*-BINAPO)](hfa = hexafluoroacetylacetonate) (where Ln = Yb, Eu) were synthesized. The complex, [Eu(TFN)$_3$(*S*-BINAPO)] gives strong red emission at 615 nm with narrow emission band (<10 nm) when excited by 465 nm light with quantum efficiency 86%. The dissymmetry factors ($g = \Delta\varepsilon_{ext}/\varepsilon_{max}$) corresponding to the $^7F_1 \rightarrow {}^5D_0$ transition at 590 nm is 0.091 for [Eu(TFN)$_3$(*S*-BINAPO)] and for [Yb(hfa)$_3$(*S*-BINAPO)](hfa = hexafluoroacetylacetonate) corresponding to the $^2F_{7/2} \rightarrow {}^2F_{5/2}$ transitions is 0.12, are among the largest values for both Eu and Yb complexes to date, respectively. The Eu complexes, [Eu(HFT)$_3$(*S*-BINAPO)] and [Eu(TFN)$_3$(*S*-BINAPO)] are found to be spontaneously emissive, showing bright red emission, when placed in sunlight or even in the laboratory when light is switched on.

1. Introduction

Chiral as well as luminescent lanthanide complexes are of value for their applications in both material and life science. Chiral lanthanide complexes with large dissymmetry factors ($g = \Delta\varepsilon_{ext}/\varepsilon_{max}$) may represent stereo-discriminating probes in biological media, due to the luminescent properties of the most rare-earth ions [1a]. Highly emissive and enantiopure lanthanide complexes have been used as cellular imaging and reactive probes by their interactions with DNA [1b]. Deployment of chiral lanthanide complexes as catalysts for various asymmetric synthesis has also been received much awareness [2]. Europium(III) complexes have been regarded as attractive for use as luminescent materials because of their red emissions (615 nm) [3]. Characteristic red emissions of Eu(III) complexes emerge from both the magnetic dipole transitions to $^7F_1$ (orange-red) and the electric dipole transitions to $^7F_2$ [4]. Magnetic dipole transitions are allowed, which makes them having approximately the same intensity as the forbidden electric dipole transitions with the exception of the hypersensitive transitions, which due to the vibronic mixing, have the large intensity. Transition from the 4f inner shell of free Eu(III) is forbidden because it does not associate with the change of parity. However, transitions that are forbidden by odd parity become partially allowed by mixing 4f and 5d states through ligand field effects of Eu(III) complexes [5]. An important point of the studies is to determine how the electron transitions in Eu(III) can be controlled by the molecular design of Eu(III) complexes. Population inversion in 4f orbitals in Ln(III) complexes is a great benefit in the development of organic chelate laser and plastic optical fiber applications [4,6]. Eu(III) complexes with higher emission quantum yields and faster radiation rates than conventional Eu(III) complexes have been designed [7]. Eu(III) complexes that exhibit both high emission quantum yields and fast radiation rates are desirable luminescent materials for laser and fiber applications. Thus, Eu(III) complexes are designed to meet several conditions: (1) higher emission quantum yields to increase ρ_s (energy density) values (2) faster radiation rates to produce large *B* (Einstein coefficient) values and (3) large dissymmetry factors for chiral discrimination. Eight coordinated Eu(III) complexes with square anti prism (SAP) geometry may generate stronger electric

* Corresponding author. Tel.: +880 821 713491x151; fax: +880 821 715257.
E-mail address: subhan-che@sust.edu (M.A. Subhan).

0020-1693/$ - see front matter © 2008 Elsevier B.V. All rights reserved.
doi:10.1016/j.ica.2008.03.093

dipole radiation through suitable ligand field effects. SAP structured Eu(III) complexes are expected to have increased radiation rates and quantum yields because of the increases in $^5D_0 \rightarrow {}^7F_2$ emissions (electronic dipole transition), related to odd parity. Phosphine oxide ligands can produce antisymmetrical structures that promote faster radiation rates. Furthermore, increased emission quantum efficiency of Eu(III) complexes can be expected, because the coordination of phosphine oxide moiety (1) prevents the coordination of water or solvent molecules and (2) lowers vibrations (P=O:1125 cm^{-1}) [7]. The BINAPO ligand is anticipated to offer dissymmetric environment to the Eu(III) ion causing an increase in the electron transition probability ($^5D_0 \rightarrow {}^7F_2$ transition) in the 4f orbitals due to odd parity. In the present study we describe the synthesis, characterization and chiral as well as luminescent properties of lanthanide (Eu(III) and Yb(III)) complexes [8] with a BINAPO ligand (see Scheme 1).

2. Experimental

2.1. Chemicals and reagents

Europium and ytterbium acetate monohydrate (99.9%), 1,1,1,5,5,5-hexafluoro-2,4-pentanedione (HFA), were purchased from Wako Pure Chemical Industries Ltd., 4,4,4-trifluoro-1(2-napthyl)-1,3-butanedione and 4,4,5,5,6,6,6-heptafluoro-1-(2-thienyl)-1, 3-hexanedione were purchased from Aldrich Chemical Co. and Acros Organics Co., respectively. BINAP was purchased from Wako Pure Chemical Industries Ltd. All chemicals and reagents were of analytical grade and used as received.

2.2. Synthesis and characterization of the complexes

The *S*-BINAPO ligand was prepared by the oxidation of BINAP [9] with H_2O_2 in THF at 0 °C for 12 h. The ligand was characterized by IR, NMR and elemental analysis. ^1H NMR (acetone-d_6, TMS) peaks were obtained at δ 6.63 (d, 2H), δ 6.77 (t, 2H), δ 7.30–7.36 (m, 8H), δ 7.38–7.50 (m, 12H), δ 7.79–7.87 (q, 4H), δ 7.88–7.91 (d, 2H) and δ 7.93–7.96 (d, 2H) ppm. The elemental analysis of *S*-BINAPO ligand was performed, found: C, 80.72; H, 4.89 and Calc. for $C_{44}H_{32}O_2P_2$: C, 80.75; H, 5.03%.

2.3. Synthesis of lanthanide complexes

2.3.1. Synthesis of $Ln(HFA)_3$ and $Ln(HFT)_3$ (Ln = Eu, Yb)

$Ln(HFA)_3$ and $Ln(HFT)_3$ (Ln = Eu, Yb) were synthesized by dissolving europium or ytterbium acetate monohydrate in ethanol in a baker and then adding slowly the ethanol solution of HFA or HFT with stirring in an ice bath (~1:3 molar ratio). Ligand TFN was dissolved in a mixed solvent of methanol and ethanol and then added to ethanol solution of $Ln(acetate)_3$ (~1:3 molar ratio) with stirring in an ice bath to synthesise $Ln(TFN)_3$. A representative synthesis of $Eu(HFT)_3$ is described here. Europium acetate monohydrate (5.0 g, 12.5 mmol) was dissolved in 20 mL ethanol in a beaker by stirring at 0 °C. Then a solution of HFT (10.8 g, 33.6 mmol) in 5 mL methanol was added dropwise to the above solution with continuous stirring. A white yellow precipitate was obtained after 2 h. The reaction mixture was filtered and air dried (% yield, 70%).

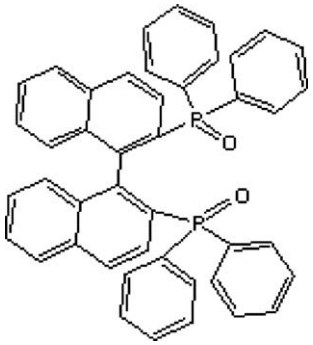

Scheme 1. Schematic diagram of BINAPO ligand.

2.3.2. Synthesis of $[Eu(HFA)_3(S\text{-}BINAPO)]$, $[Eu(HFT)_3(S\text{-}BINAPO)]$ and $[Eu(TFN)_3(S\text{-}BINAPO)]$

An acetone solution (200 mL) containing $Eu(HFA)_3$, $Eu(HFT)_3$ or $Eu(TFN)_3$ and BINAPO ligand (1:1 molar ratio) was refluxed at ~50 °C for 10 h with continuous stirring to obtain a clear solution of desired complexes $[Eu(HFA)_3(S\text{-BINAPO})]$, $[Eu(HFT)_3(S\text{-BINAPO})]$ or $[Eu(TFN)_3(S\text{-BINAPO})]$, respectively. In each case, the resulting mixture was concentrated and hexane was added to it, which gave crystalline precipitate. For an example synthesis of $[Eu(TFN)_3(S\text{-BINAPO})]$ is given here. $[Eu(TFN)_3] \cdot 2H_2O$ (5.35 g, 1 mmol) was dissolved in 200 mL acetone in a round bottom flask. Then (3 g, 1 mmol) of *S*-BINAPO was added to the above solution. A turbid mixture obtained was shaken and a clear solution was obtained in a few minutes. This solution was refluxed for 10 h. The resulting mixture was concentrated and hexane was added. A yellow crystalline solid obtained was filtered and dried in air (% yield, 60%). The single crystals of these complexes were grown by recrystallization from toluene–cyclohexane mixed solvent for a few days. The needle like crystal was mounted on a capillary but decomposes in the course of X-ray analysis. The complexes $[Yb(HFA)_3(S\text{-BINAPO})]$, $[Yb(HFT)_3(S\text{-BINAPO})]$ and $[Yb(TFN)_3(S\text{-BINAPO})]$ were also synthesized by the same procedure as described for the corresponding Eu(III) complexes. Single crystals of $[Yb(HFA)_3(S\text{-BINAPO})]$ were grown by recrystallization from toluene–cyclohexane mixed solvent for several days. Elemental analysis for the following complexes was performed, results are as given below: *Anal.* Calc. for $C_{90}H_{56}O_8F_9P_2Eu$ $[Eu(TFN)_3\ (S\text{-BINAPO})]$: H, 3.42; C, 65.50. Found: H, 3.62; C, 65.49%. *Anal.* Calc. for $C_{90}H_{56}O_8F_9P_2Yb$ $[Yb(TFN)_3(S\text{-BINAPO})]$: H, 3.38, C, 64.68. Found: H, 3.58; C, 64.65%. *Anal.* Calc. for $C_{59}H_{35}O_8F_{18}P_2Yb \cdot C_6H_{14}$ $[Yb(HFA)_3(S\text{-BINAPO})] \cdot C_6H_{14}$: H, 3.22, C, 50.86. Found: H, 2.80; C, 50.70%. *Anal.* Calc. for $C_{70}H_{48}O_{10}F_{21}S_3PEu$ $[Eu(HFT)_3(S\text{-BINAPO})]$: H, 2.75; C, 47.82. Found: H, 2.41; C, 48.82%. The ESI-MS data were collected for $[Yb(HFA)_3(S\text{-BINAPO})]$ and $[Yb(TFN)_3(S\text{-BINAPO})]$ complexes. For $[Yb(HFA)_3(S\text{-BINAPO})]$, m = 1449, m/z 1242, $[1449-hfa]^+$; m/z 1896, $[1449-hfa+BINAPO]^+$ and $[Yb(TFN)_3(S\text{-BINAPO})]$, m = 1623, m/z 655, $BINAPO+H^+$; m/z 1358, $[M-TFN]^+$; m/z 2012, $[M-TFN+BINAPO]^+$ were obtained.

Other complexes, $[Ln(TFN)(HBpz_3)_2]$, $[Ln(HFT)(HBpz_3)_2]$, $[Ln(HFA)\ (HBpz_3)_2]$ and $[Ln(TFN)_2(HBpz_3)]$, $[Ln(HFT)_2(HBpz_3)]$ (Ln = Eu, Ce and $HBpz_3^- =$ Hydrotris(pyrazole-1-yl)borate) were synthesized by dissolving respective hydrated salts of $Ln(NO_3)_3$ or $LnCl_3$ into water and then adding simultaneously an aqueous solution of $HBpz_3$ and ethanol solution of TFN, HFT or HFA to the above aqueous solution in a beaker, respectively. In each case, mixing of solutions following stirring for 15 min produced precipitates of Ln-complexes, which were subsequently filtered, air-dried and characterized by IR.

2.4. Measurements

For measuring the spectra in solution lanthanide complexes were dissolved in acetone. Absorption spectra were measured on a Perkin–Elmer Lambda-19 spectrophotometer. CD data were collected on a Jasco J-720W spectropolarimeter. Infrared spectra were obtained with a Perkin–Elmer FT-IR 2000 spectrometer. Elemental analyses were performed with a Perkin–Elmer 240C. Emission

spectra were measured at room temperature using a HITACHI F-4500 system. The spectra were corrected for detector sensitivity and lamp intensity variations. Quantum efficiency was determined using a standard integrating sphere (diameter 6 cm) [10].

2.5. Crystal structure determination

A colorless needle crystal of complex [Yb(HFA)$_3$(*S*-BINAPO)] was sealed in a glass capillary tube to prevent possible efflorescence. The X-ray intensities ($2\theta_{max} = 60°$) were measured on a Rigaku AFC-5R, and absorption corrections were made by either the empirical Ψ-scan method [11] or the numerical integration method [12]. The structure was solved by the direct method using SHELXS 86 program [13], and refined on F^2 against all the reflections by the full matrix least-squares technique using anisotropic thermal parameters for all non-hydrogen atoms. Hydrogen atoms were placed at the positions generated by theoretical calculations and fixed during the structural refinement cycles. All the calculations were carried out using a TEXSAN software package [14]. The ORTEP [15] view of the complex is shown in Fig. 1.

3. Results and discussion

The complexes were synthesized and characterized by elemental analysis, FT-IR, ESI-MS and X-ray. The IR spectra for the complex, [Eu(TFN)$_3$(*S*-BINAPO)] (Fig. S1), show characteristic peaks. In addition to the satisfactory results from the elemental analysis, IR, ESI-MS and finally the structure was confirmed by X-ray analysis. The complexes were found to be highly soluble in acetone and moderately soluble in water.

3.1. X-ray analysis

The crystallographic data are shown in Table 1 and the selected bond lengths and angles are summarized in Table 2. The complex [Yb(HFA)$_3$(*S*-BINAPO)] crystallizes in monoclinic crystal system with P_12_{11} space group. This complex indicates the effective eight coordination with six oxygens from three HFA ligands and two oxygen from BINAPO to the Yb(III) ions in [Yb(HFA)$_3$ (*S*-BINAPO)], forming the square antiprism as shown in Fig. 1. The R_w value was found to be 0.2807 as shown in Table 1. Two crystallographically

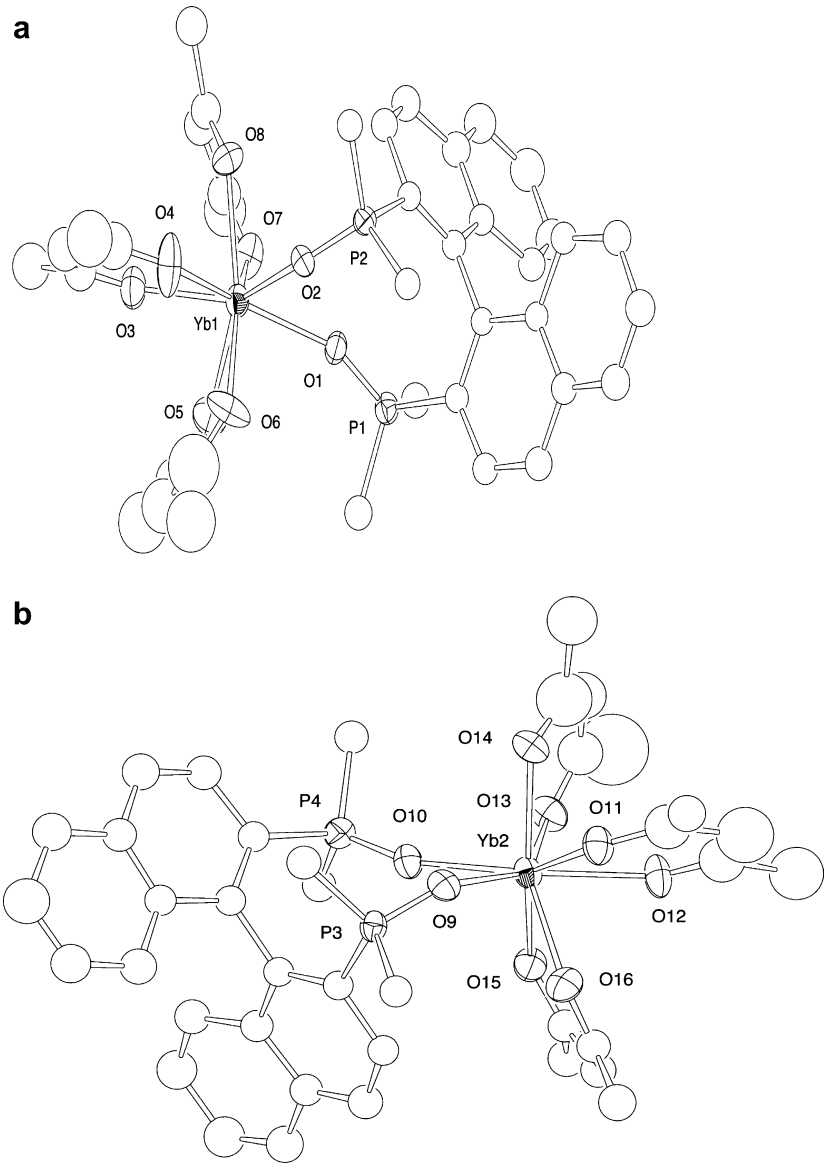

Fig. 1. Ortep view of two crystallographically independent complexes of [Yb(HFA)$_3$(*S*-BINAPO)] (phenyl rings are omitted for clarity).

Table 1
Crystallographic data for [Yb(HFA)$_3$(*S*-BINAPO)]

Formula	$C_{59}H_{35}F_{18}O_8P_2Yb$
M	1448.85
T (K)	293(2)
λ(Mo Kα)/Å	0.71069
Crystal system	monoclinic
Space group	P_12_{11}
a (Å)	13.9079(5)
b (Å)	18.1271(7)
c (Å)	26.9541(10)
α (°)	90.00
β (°)	93.6170(10)
γ (°)	90.00
V (Å^3)	6781.9(4)
Z	4
$\rho_{calc.}$ (g cm^{-3})	1.419
μ(Mo Kα) (cm^{-1})	1.522
R_1 (F^2)	0.1033
wR_2 (F^2)	0.2807

Table 2
Selected bond length (Å) and bond angles (°) of [Yb(HFA)$_3$ (BINAPO)]

Bond length			
Yb1 O2	2.229(8)	Yb2 O15	2.299(10)
Yb1 O6	2.261(13)	Yb2 O16	2.331(11)
Yb1 O1	2.272(9)	Yb2 O13	2.351(10)
Yb1 O7	2.294(12)	Yb2 O11	2.403(10)
Yb1 O3	2.300(10)	Yb2 P3	3.534(3)
Yb1 O8	2.330(9)	P1 O1	1.480(9)
Yb1 O5	2.340(10)	P2 O2	1.481(8)
Yb1 O4	2.339(13)	P3 O9	1.482(10)
Yb1 C53	3.15(6)	P3 C72	1.786(14)
Yb2 O9	2.235(9)	P3 C60	1.785(16)
Yb2 O14	2.282(11)	P3 C66	1.783(15)
Yb2 O12	2.288(9)	P4 O10	1.477(11)
Yb2 O10	2.304(10)		
Bond angle			
O2 Yb1 O6	79.7(4)	O10 Yb2 O15	76.9(4)
O2 Yb1 O1	76.5(3)	O9 Yb2 O16	76.2(4)
O6 Yb1 O1	89.1(5)	O14 Yb2 O16	139.7(4)
O2 Yb1 O7	123.1(4)	O12 Yb2 O16	78.1(5)
O6 Yb1 O7	146.9(5)	O10 Yb2 O16	120.3(4)
O1 Yb1 O7	75.5(4)	O15 Yb2 O16	71.5(4)
O2 Yb1 O3	142.3(4)	O9 Yb2 O13	144.3(4)
O6 Yb1 O3	101.9(5)	O14 Yb2 O13	73.4(4)
O1 Yb1 O3	140.7(4)	O12 Yb2 O13	71.8(4)
O7 Yb1 O3	75.1(5)	O10 Yb2 O13	73.7(4)
O2 Yb1 O8	76.2(3)	O15 Yb2 O13	72.6(4)
O6 Yb1 O8	140.7(5)	O16 Yb2 O13	136.3(4)
O1 Yb1 O8	114.5(4)	O9 Yb2 O11	73.4(4)
O7 Yb1 O8	72.1(4)	O14 Yb2 O11	69.0(4)
O3 Yb1 O8	80.0(4)	O12 Yb2 O11	70.9(4)
O2 Yb1 O5	141.4(4)	O10 Yb2 O11	143.2(4)
O6 Yb1 O5	71.5(5)	O15 Yb2 O11	136.1(4)
O1 Yb1 O5	77.9(4)	O16 Yb2 O11	70.9(4)
O7 Yb1 O5	76.7(5)	O13 Yb2 O11	124.9(4)
O3 Yb1 O5	70.4(5)	O9 Yb2 P3	14.5(3)
O8 Yb1 O5	141.4(4)	O14 Yb2 P3	100.2(3)
O2 Yb1 O4	74.6(4)	O12 Yb2 P3	148.0(3)
O6 Yb1 O4	71.4(7)	O10 Yb2 P3	66.9(3)
O1 Yb1 O4	147.5(4)	O15 Yb2 P3	103.7(3)
O7 Yb1 O4	133.9(5)	O16 Yb2 P3	73.2(3)
O3 Yb1 O4	70.5(4)	O13 Yb2 P3	140.0(3)
O8 Yb1 O4	72.5(6)	O11 Yb2 P3	86.1(3)
O5 Yb1 O4	117.6(6)	C112 Yb2 P3	115.7(8)
O9 Yb2 O14	88.9(4)	P2 O2 Yb1	145.7(6)
O9 Yb2 O12	141.2(4)	P3 O9 Yb2	143.2(6)
O14 Yb2 O12	92.4(4)	P4 O10 Yb2	163.8(7)
O9 Yb2 O10	75.8(4)		
O14 Yb2 O10	90.8(4)		
O12 Yb2 O10	142.8(4)		
O9 Yb2 O15	117.7(4)		
O14 Yb2 O15	145.8(4)		
O12 Yb2 O15	80.0(4)		

independent complexes, which corresponded to Δ-[Yb(HFA)$_3$-(*S*-BINAPO)] and Λ-[Yb(HFA)$_3$(*S*-BINAPO)], in which Yb–O bond lengths are between 2.23 and 2.4 Å in the Yb-moiety. These bond lengths are very similar to that found for mononuclear Δ-[Yb(HBpz$_3$)$_2$(*S*-pba)], Λ-[Yb(HBpz$_3$)$_2$(*S*-pba)] and dinuclear (Λ–Δ)-Cr(ox)Yb [16]. This results indicate effective coordination of oxygen ligands from either BINAPO or HFA to Yb(III). Bond angle, O2 Yb1 O1 is 76.5(3)° and O9 Yb2 O10 is 75.8(4)° as shown in Table 2. These values are comparable to that observed for (Λ–Δ)-Cr(ox)-Yb (70.9(5)°) but much smaller than that observed for either Δ-[Yb(HBpz$_3$)$_2$(*S*-pba)] (55.5(1)°) or Λ-[Yb(HBpz$_3$)$_2$(*S*-pba)] (55.6(1)°) [16]. The coordination environment around the Yb(III) is seems to be similar to that of dinuclear, Cr(ox)Yb, which was found to be configurationally chiral with the retention of chirality [16]. Furthermore, the SAP structure of [Yb(HFA)$_3$(*S*-BINAPO)] is analogous to mononuclear (BIPHEPO)Eu(hfa)$_3$ with more dissymmetry to the Yb(III) exerted by BINAPO ligand [17].

3.2. CD spectra analysis

3.2.1. CD spectra of [Eu(TFN)$_3$(*S*-BINAPO)]

The Eu(III) complex gives sharp electronic transitions at $^7F_0 \rightarrow {}^5D_0$, $^7F_0 \rightarrow {}^5D_j$ and $^7F_j \rightarrow {}^5D_0$ ($J = 0$, 1 or 2). We studied the CD spectral features of the f–f transitions of [Eu(TFN)$_3$(*S*-BINAPO)] in order to reveal the nature of formally forbidden transition with $|\Delta J| = 0$, $|\Delta J| = 1$, magnetic dipole transition and the electric dipole transition, $|\Delta J| = 2$, respectively. For a clear observation of the circular dichoric f–f transitions of Eu(III), optically active and sterically bulky enantiopure BINAPO ligand was chosen to induce the configurational chirality around the Eu(III). For the complex, [Eu(TFN)$_3$-(*S*-BINAPO)], the CD bands corresponding to the electric dipole transitions, $^7F_1 \rightarrow {}^5D_1$, $^7F_0 \rightarrow {}^5D_1$ and $^7F_0 \rightarrow {}^5D_2$ was observed at around 540 nm ($|g| = 0.0014$), 525 nm ($|g| = 0.04$) and 465 nm ($|g| = 0.001$), respectively, as shown in Fig. 2. Moreover, a prominent CD signal corresponding to magnetic dipole transition,

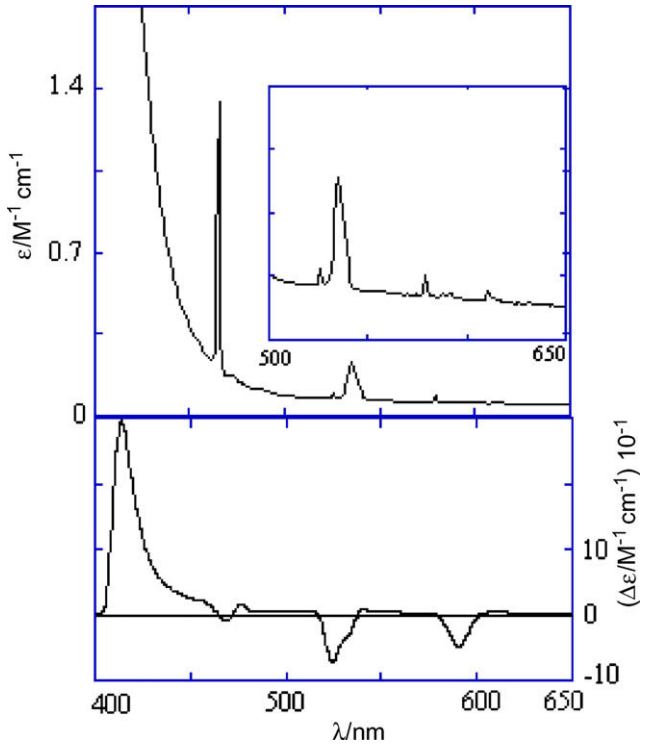

Fig. 2. Absorption and circular dichroism (CD) spectra of complex [Eu(TFN)$_3$(*S*-BINAPO)].

$^7F_1 \rightarrow {}^5D_0$ was observed at around 590 nm with a dissymmetry factor of ($|g| = 0.091$). This is the largest value of the dissymmetry factors for Eu(III) known to date (Fig. 2), which is close to that observed for CPL spectra of a Eu(III) complex, for sensitive transitions $^5D_0 \rightarrow {}^7F_1$ ($g_{em} = -0.088$) [18]. This large dissymmetry factor [16,19] indicates that the configurational chirality is induced by BINAPO around the Eu(III). CD signal corresponding to the $^7F_0 \rightarrow 5D_0$ was not clearly observed. This transition is formally forbidden but it is in fact allowed by *J* mixing with the neighboring electronic transitions. The CD silent $^7F_0 \rightarrow {}^5D_0$ transitions may be attributed to a lack of the magnetic transition moment upon transition, for which the much smaller *J* mixing of the magnetic and electric dipole moments upon CD transition would be responsible. This seems to be reasonable, since CD transition is affected in principle by the angular momentum and the total angular momentum of both the ground state ($^7F_0$) and excited state ($^5D_0$) is absolutely zero for the particular transition, $^7F_0 \rightarrow {}^5D_0$. Furthermore, a CD band corresponding to electric dipole transition was observed at 615 nm ($|g| = 0.01$). The CD bands corresponding to the $^7F \rightarrow {}^5D$ transitions, from the different levels of ground $^7F_0$ to that of excited ^5D within the f^6 configurations of Eu(III) chromophore are schematically presented in Fig. 3. The $^7F \rightarrow {}^5D$ transitions of Eu(III) may be classified into two categories in terms of angular momentum change, the magnetic dipole allowed and electric dipole allowed. It is noted that among these transitions $^7F_1 \rightarrow {}^5D_0$, which involve the magnetic dipole change gives dissymmetry factor *g*, much larger than that observed for the corresponding electric dipole transitions, $^7F_2 \rightarrow {}^5D_0$(615 nm), $^7F_0 \rightarrow {}^5D_2$(465 nm), and the CD silent transition $^7F_0 \rightarrow {}^5D_0$. These results indicate that the magnetic dipole, rather than the electric dipole transitions enhance the *J* mixing and eventually giving rise to a stronger CD signal, for the transitions accompanying an angular momentum change. The small dissymmetry factor observed for transitions at around 530 and 540 nm might be due to the larger mixing between magnetic dipole $^7F_0 \rightarrow {}^5D_1$ and allowed transition $^7F_1 \rightarrow {}^5D_1$, which finally shows lessening of CD intensity due to the mutual cancellation. The similar CD behaviors are observed for other configurationally chiral lanthanide complexes [16,19].

3.2.2. CD spectra of [Yb(TFN)$_3$(S-BINAPO)] and [Yb(HFA)$_3$(S-BINAPO)]

The unique f–f transitions of Yb(III) from ground states $^2F_{7/2}$ to excited state $^2F_{5/2}$ are split by the crystal field into four and three doubly degenerate sublevels, respectively. This is magnetically allowed ($\Delta J = 1$) and can be classified among the most CD sensitive of the rare-earth series [20]. Due to the small energy difference between states of the lower terms (of the order of 10^2 cm^{-1}), a temperature-reliant Boltzmann distribution of the populations of four states of ground $^2F_{7/2}$ state is predictable. Accordingly, up to 12 transitions might be observable about the center of gravity. For each of the Yb(III) complexes with in f^{13} electronic configuration, five CD bands were merely observed at around 927 nm, 945 nm, 960 nm, 975 nm and 995 nm as shown in Fig. 4. The dissymmetry

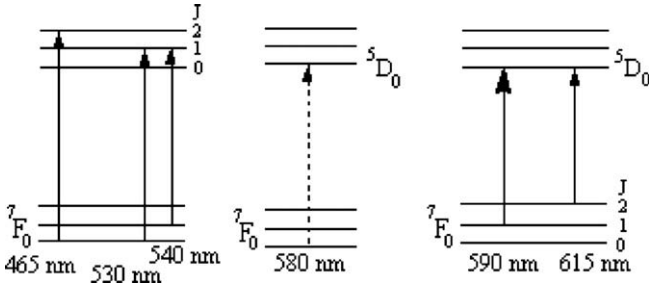

Fig. 3. Schematic diagram of f–f transitions of Eu(III) in [Eu(TFN)$_3$(*S*-BINAPO)].

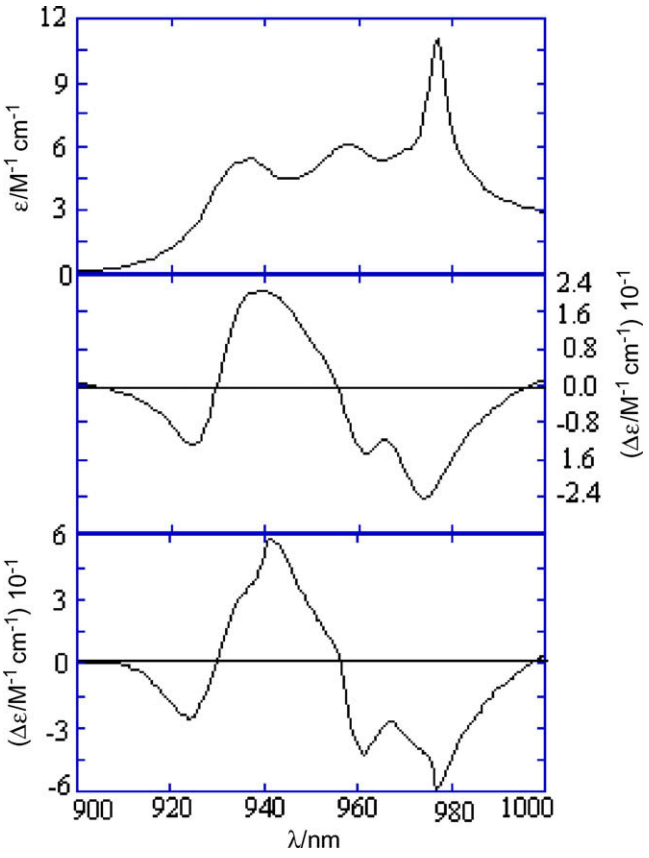

Fig. 4. Absorption (top) and CD (middle) spectra of complex [Yb(TFN)$_3$(*S*-BINAPO)] and CD spectra (bottom) of [Yb(HFA)$_3$(*S*-BINAPO)].

factors ($|g|$) for [Yb(TFN)$_3$(*S*-BINAPO)] and [Yb(HFA)$_3$(*S*-BINAPO)] complexes corresponding to bands at 945 nm, 960 nm, 975 nm, are found to be 0.036, 0.12; 0.02, 0.075 and 0.061, 0.023, respectively. These large dissymmetry factors indicate configurational chirality around the Yb(III) ion [16,21]. These multiple CD components in both the complexes arise from the ligand field splitting within the $^2F_{7/2} \rightarrow {}^2F_{5/2}$ transitions of the Yb(III) chromophores. These are expected to be few transitions from four Kramers doublets of the ground $^2F_{7/2}$ states to three of the excited $^2F_{5/2}$ states, as schematically shown in Fig. 5, where positive and negative signs refer to the CD sign.

Either [Eu(TFN)$_3$(*S*-BINAPO)] or [Yb(TFN)$_3$(*S*-BINAPO)] and [Yb(HFA)$_3$(*S*-BINAPO)] complexes are highly soluble in acetone and moderately soluble in water. CD intensities as well as CD signs

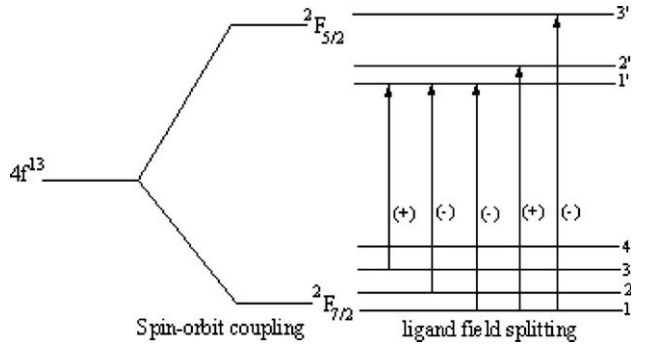

Fig. 5. Schematic diagram of transitions from four Kramers doublets of the ground $^2F_{7/2}$ states to three of the excited $^2F_{5/2}$ states of Yb(III) ions and positive and negative signs from left to right refer to the CD signs from the longer wavelength side.

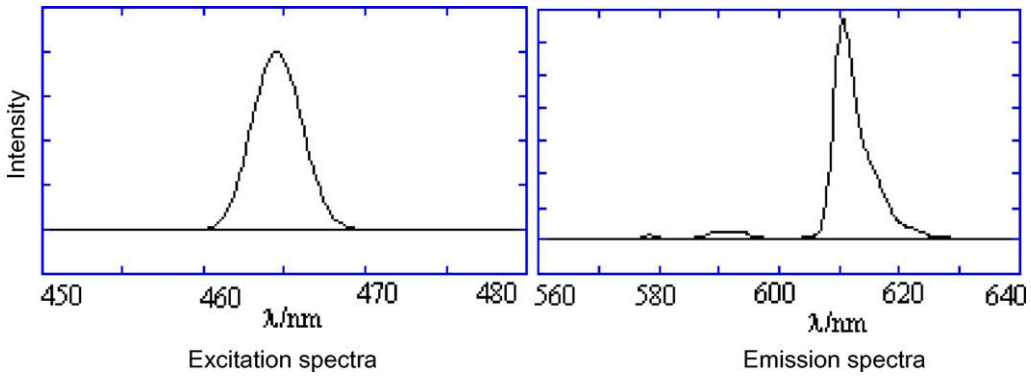

Fig. 6. Excitation and emission spectra of [Eu(TFN)$_3$(*S*-BINAPO)].

were found to remain unchanged on standing for several days in acetone solution. For these *S*–BINAPO complexes negative sign corresponding to major CD bands indicates preference of Λ isomer in solution as shown in Figs. 2 and 4, respectively [19]. However, on long standing change in CD intensities as well as CD signs may be attributed to ligand scrambling in the solution and presence of mixtures of fluxional complexes in equilibrium.

3.3. Luminescent properties

The Eu complexes were found to be naturally and spontaneously emissive, showing bright red emission (at 615 nm), when placed in sunlight or even in the laboratory when light is switched on. Emission bands were observed at around 580, 590, 615, 650, and 700 nm, and are attributed to the f–f transitions $^5D_0 \rightarrow {}^7F_J$ (J = 0, 1, 2, 3 and 4, respectively) when excited at 465 nm. The strongest emission band at around 615 nm ($^5D_0 \rightarrow {}^7F_2$) was due to the electronic dipole transition as shown in Fig. 6 [7,17]. The similar complexes without BINAPO ligand are not naturally emissive but these show emissions, when irradiated by UV–vis light. For example, we synthesized similar complexes of Eu(III) and Ce(III); [Ln(TFN)$_3$], [Ln(HFT)$_3$], [Ln(HFA)$_3$] and [Ln(TFN)(HBpz$_3$)$_2$], [Ln(HFT)(HBpz$_3$)$_2$], [Ln(HFA)(HBpz$_3$)$_2$] and [Ln(TFN)$_2$(HBpz$_3$)], [Ln(HFT)$_2$(HBpz$_3$)](HBpz$_3^-$ = Hydrotris(pyrazole-1-yl)borate), without BINAPO ligand, which are not spontaneously emissive but show characteristics emissions when irradiated by UV–vis light at 380 nm by a mercury lamp. The strong red emission with narrowed band (half width <10 nm) of complexes [Eu(TFN)$_3$(*S*-BINAPO)] and [Eu(HFT)$_3$(*S*–BINAPO)] were observed by excitation at 465 nm. The emission quantum efficiency was calculated to be 86% for [Eu(TFN)$_3$(*S*–BINAPO)], which is very close to that observed for Eu(hfa)$_3$(BIPHEPO) (87%) [17].

4. Conclusions

The lanthanide complexes described here show promising chiral as well as luminescent behavior. The complex, [Eu(TFN)$_3$(*S*-BINAPO)], provides strong red emission at 615 nm with narrow emission band (<10 nm) when excited by 465 nm light with quantum efficiency 86%. The Eu(III) complexes are found to be spontaneously emissive, showing bright red emission, when placed in sunlight or even in the laboratory when light is switched on. The Eu(III) and Yb(III) complexes, [Eu(TFN)$_3$(*S*-BINAPO)], [Yb(TFN)$_3$(*S*-BINAPO)] and [Yb(HFA)$_3$(*S*–BINAPO)] show remarkable chirality with high dissymmetry factors. The dissymmetry factors ($g = \Delta\varepsilon_{ext}/\varepsilon_{max}$) corresponding to the $^7F_1 \rightarrow {}^5D_0$ transition at 590 nm is 0.091 for [Eu(TFN)$_3$(*S*-BINAPO)] and 0.12 for [Yb(hfa)$_3$(*S*–BINAPO)](hfa = hexafluoroacetylacetonate) corresponding to the $^2F_{7/2} \rightarrow {}^2F_{5/2}$ transitions, are among the largest values for both Eu and Yb complexes to date, respectively. Further investigations on spectroscopic and photo-physical properties of complexes are a requirement for their potential applications in material as well as life sciences.

Acknowledgements

Venture business laboratory (VBL) of Osaka University is gratefully acknowledged for providing a postdoctoral fellowship to Dr. Md. Abdus Subhan for a year during this work. Thanks to Dr. Nobuko Kanehisa, Department of Material and Life Science, Division of Advanced Science and Biotechnology, Graduate School of Engineering, Osaka University, 2-1 Yamada-oka, Suita, Osaka 565-0871, Japan, for her cooperation during X-ray measurements.

Appendix A. Supplementary data

Supplementary data associated with this article can be found, in the online version, at doi:10.1016/j.ica.2008.03.093.

References

[1] (a) D. Parker, J.A.G. Gareth Williams, J. Chem. Soc., Dalton Trans. (1996) 3613;
(b) J.C. Frias, G. Bobba, M.J. Cann, C.J. Hutchison, D. Parker, Org. Biol. Chem. 1 (2003) 905.
[2] T. Hayano, T. Sakaguchi, H. Furuno, M. Ohba, H. Okawa, J. Inanaga, Chem. Lett. 32 (7) (2003) 608.
[3] G. Blasse, B.C. Grabmaier, Review on Luminescence Behaviors: Luminescent Materials, Springer-Verlag, New York, 1994.
[4] F. Gan, Laser Materials, World Scientific, Singapore, 1995. p. 70.
[5] Selected papers of luminescent Eu(III) complexes: (a) L. Charbonniere, R. Ziessel, M. Guardigli, A. Roda, N. Sabbatini, J. Am. Chem. Soc. 123 (2001) 2436;
(b) X. Yang, C. Su, B. Kang, X. Feng, W. Xiao, H. Liu, J. Chem. Soc., Dalton Trans. 19 (2000) 3253;
(c) H. Son, J. Roh, S. Shin, J. Park, J. Ku, J. Chem. Soc., Dalton Trans. 9 (2001) 1524;
(d) J.I. Bruce, R.S. Dickins, L.J. Govenlock, T. Gunnlaugsson, S. Lopinski, M.P. Lowe, D. Parker, J.J.B. Perry, S. Aime, M. Botta, J. Am. Chem. Soc. 122 (2000) 9674;
(e) N. Fatin-Rouge, E. Toth, D. Perret, R.H. Backer, A.E. Merbach, J.G. Buenzli, J. Am. Chem. Soc. 122 (2000) 10810;
(f) H. Tsukube, M. Hosokubo, M. Wada, S. Shinoda, H. Tamiaki, Inorg. Chem. 40 (2001) 740;
(g) P.J. Skinner, A. Beeby, R.S. Dickins, D. Parker, S. Aime, M. Botta, J. Chem. Soc., Perkin Trans. 2 7 (2000) 1329;
(h) J.G. Bunzli, L.J. Charbonniere, R.F. Ziessel, J. Chem. Soc., Dalton Trans. (2000) 1917;
(i) M.D. McGehee, T. Bergstedt, C. Zhang, A.P. Saab, M.B. O'Regan, G.C. Bazan, V.I. Srdanov, A.J. Heeger, Adv. Mater. 11 (1999) 1349;
(j) D.M. Epstein, L.L. Chappell, H. Khalili, R. Supkowski, M. Horrocks, W. DeW Jr., J.R. Morrow, Inorg. Chem. 39 (2000) 2130;
(k) S.I. Klink, L. Grave, D.N. Reinhoudt, F.C.J.M. van Veggel, M.H.V. Werts, F.J. Geurts, J.W. Hofstraat, J. Phys. Chem. A 104 (2000) 5457;
(l) J.J. Lessmann, A. Horrocks, W. DeW Jr., Inorg. Chem. 39 (2000) 3114.
[6] (a) E.J. Schimitschek, E.G.K. Schwarz, Nature 196 (1962) 832;
(b) H. Samelson, C. Brecher, V. Brophy, Appl. Phys. Lett. 5 (1964) 173;

(c) T. Kobayashi, S. Nakatsuka, T. Iwafuji, K. Kuriki, N. Imai, N. Nakamoto, C.D. Claude, K. Sasaki, Y. Koike, Y. Okamoto, Appl. Phys. Lett. 71 (1997) 2421;
(d) K. Kuriki, Y. Koike, Y. Okamoto, Chem. Rev. 102 (2002) 2347.
[7] Y. Hasegawa, M. Yamamuro, Y. Wada, N. Kanehisa, Y. Kai, S. Yanagida, J. Phys. Chem. A 107 (2003) 1697.
[8] (a) M.A. Subhan, et al., 84th Annual Meeting of Chemical Society of Japan, Abstract No. 4B3-37, 2004, p. 178;
(b) Y. Hasegawa, Y. Wada, S.Yanagida, In: 21st ICP Satellite Symposium on Photochemistry and Photobiology of Complexes Including Supramolecular Systems and Coordination Compounds, Shiga, Japan, Abstr. No. V-7, 2003.
[9] Q. Lin, T.E. Long, J. Poly. Sci., Part A 38 (2000) 3736.
[10] Y. Hasegawa, K. Sogabe, Y. Wada, T. Kitamura, N. Nakashima, S. Yanagida, Chem. Lett. (1999) 35.
[11] A.C.T. North, D.C. Phillips, F.S. Mathews, Acta Crystallogr., Sect. A 24 (1968) 351.
[12] P. Choppens, L. Leiserowitz, D. Rabinovich, Acta Crystallogr. 18 (1965) 1035.
[13] G.M. Sheldrick, Acta Crystallogr., Sect. A 46 (1990) 467.
[14] Molecular Structure Corporation, Rigaku Co. Ltd., TEXSAN, Single Crystal Structure Analysis Software, version 1.9, 1998, MSC, The Woodlands, TX 77381 5209, USA, Rigaku Co. Ltd., Akishima, Tokyo 196-8666, Japan.
[15] C.K. Johnson, ORTEP II, Report ORNL-5138, Oak Ridge 407 National Laboratory, Oak Ridge, TN, 1976.
[16] M.A. Subhan, T. Suzuki, S. Kaizaki, J. Chem. Soc., Dalton Trans. (2001) 492.
[17] K. Nakamura, Y. Hasegawa, H. Kawai, N. Yasuda, N. Kanehisa, Y. Kai, T. Nagamura, S. Yanagida, Y. Wada, J. Phys. Chem. A 111 (16) (2007) 3029.
[18] M. Lama, O. Mamula, G.S. Kottas, F. Rizzo, L. De Cola, A. Nakamura, R. Kuroda, H. Stoeckli-Evans, Chem. Eur. J. 13 (2007) 7358.
[19] M.A. Subhan, T. Suzuki, S. Kaizaki, J. Chem. Soc., Dalton Trans. (2002) 1416.
[20] F.S. Richardson, Inorg. Chem. 19 (1980) 2806.
[21] L.D. Bari, G. Pintacuda, P. Salvadori, R.S. Dickins, D. Parker, J. Am. Chem. Soc. 122 (2000) 9257.